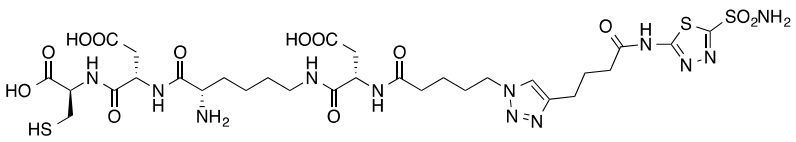

Supplemental Figure 1: ^{99m}Tc-chelating acetazolamide derivative 1

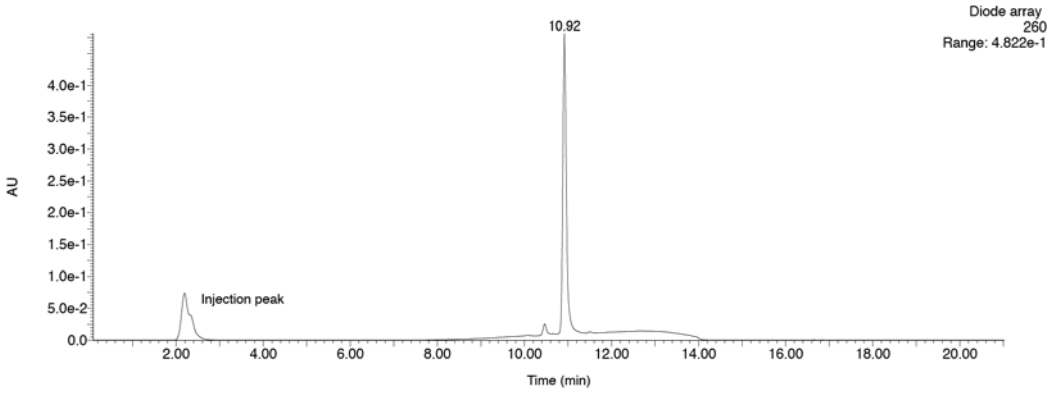

Supplemental Figure 2: Analytical HPLC trace of monovalent AAZ ^{99m}Tc ligand conjugate 1 on a Synergi RP Polar column, 5% MeCN in 0.1% aq. TFA to 80% MeCN in 20 min. Please disregard the injection peak as an artifact of the HPLC system.

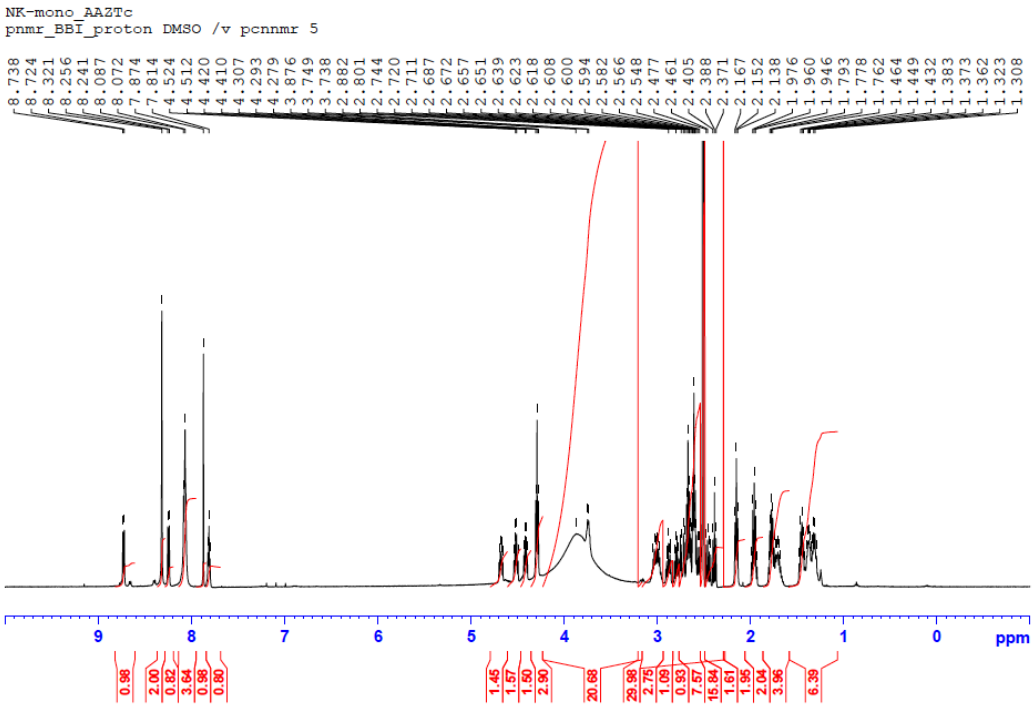

Supplemental Figure 3: ^{1}H-NMR (500 MHz) of monovalent AAZ ^{99m}Tc ligand conjugate 1 in DMSO-d_6.

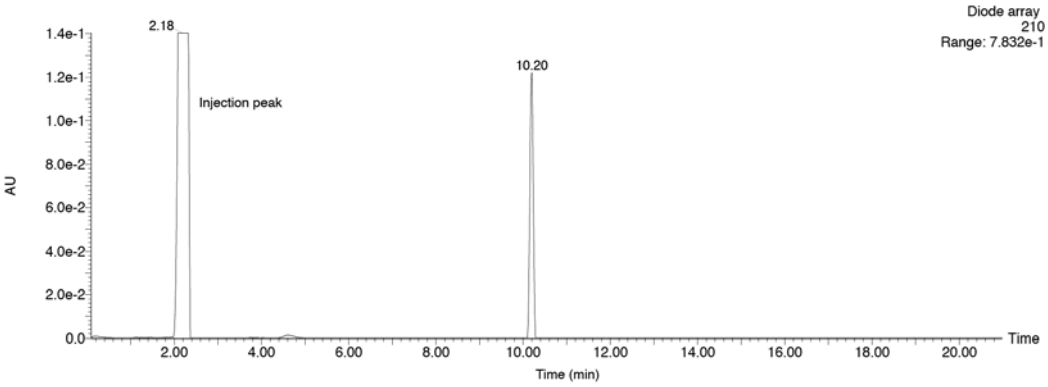

Supplemental Figure 4: Analytical HPLC trace of monovalent negative control ^{99m}Tc ligand conjugate 2 on a Synergi RP Polar column, 5% MeCN in 0.1% aq. TFA to 80% MeCN in 20 min. Please disregard the injection peak as an artifact of the HPLC system.

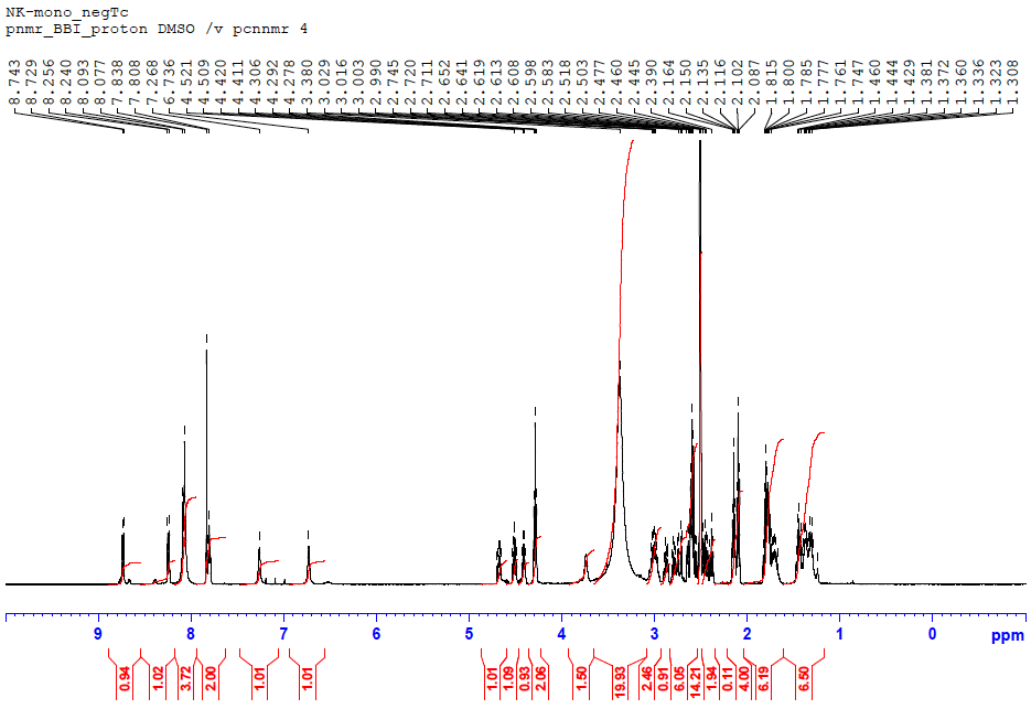

Supplemental Figure 5: ^{1}H-NMR (500 MHz) of monovalent negative control 99mTc ligand conjugate 2 in DMSO-d_6.

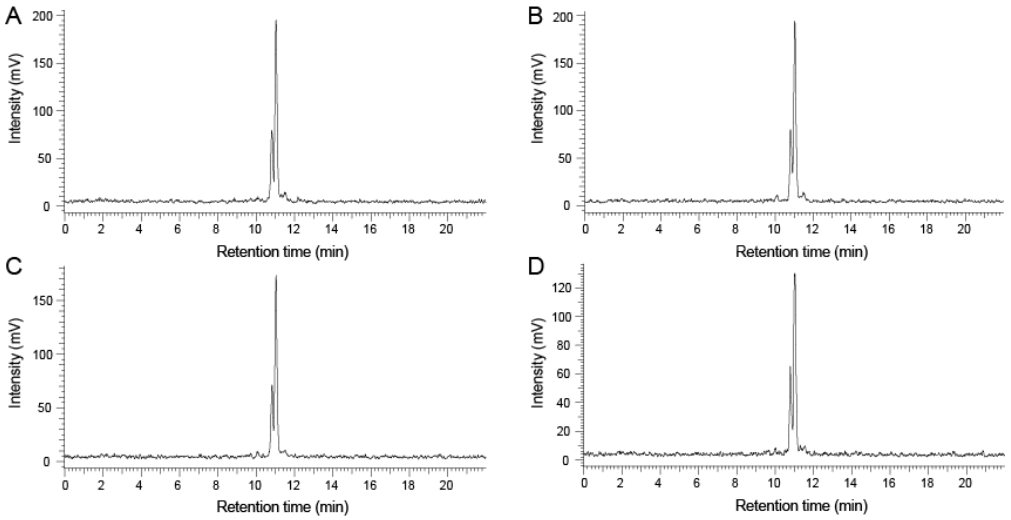

Supplemental Figure 6: Stability of ^{99m}Tc-complex of acetazolamide conjugate 1 in TBS. ^{99m}Tc-labeled preparations of 1 were incubated at the final concentration of 10 μg/mL (11 μM) in TBS. RP-HPLC chromatograms (XTerra C18, 5% MeCN in 0.1% aq. TFA to 80% over 20 min on a Merck-Hitachi D-7000 HPLC system equipped with a Raytest Gabi Star radiodetector) were recorded at 0 min (A), 10 min (B), 30 min (D) and 1 h (D). The results suggest a high stability of the ^{99m}Tc-complex of compound 1 under these experimental conditions. Double peaks reflect *syn & anti* diastereoisomers arising from two chelation poses of the ^{99m}Tc-complex (*3*).

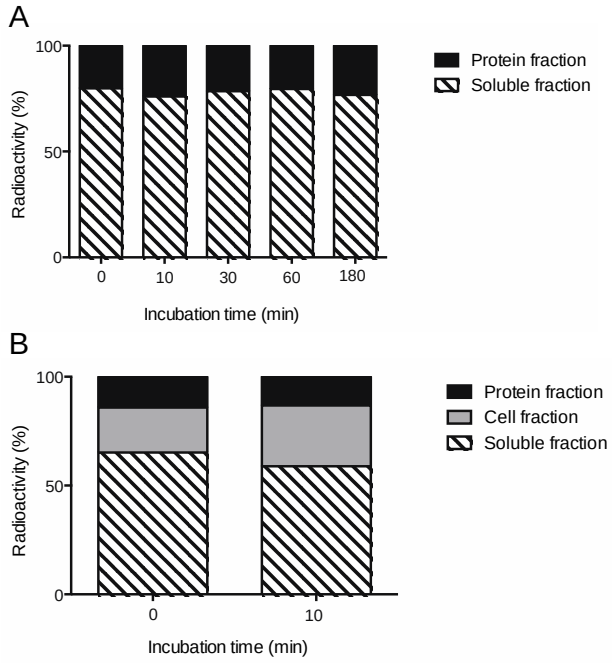

Supplemental Figure 7: Incubation experiment of ^{99m}Tc-complex of compound 1 in serum and whole blood. ^{99m}Tc-labeled preparations of 1 were incubated at the final concentration of 10µg/mL in mouse serum (A) or whole mouse blood (B). To extract the protein fraction a rapid acetonitrile-based method was used. To obtain the cellular fraction, centrifugation was applied to whole blood collected in EDTA-coated tubes. Results are presented as percentages over total measured radioactivity. The labeled preparation does not significantly bind blood cells in mice and the majority of radioactivity can be recovered in the soluble fraction.

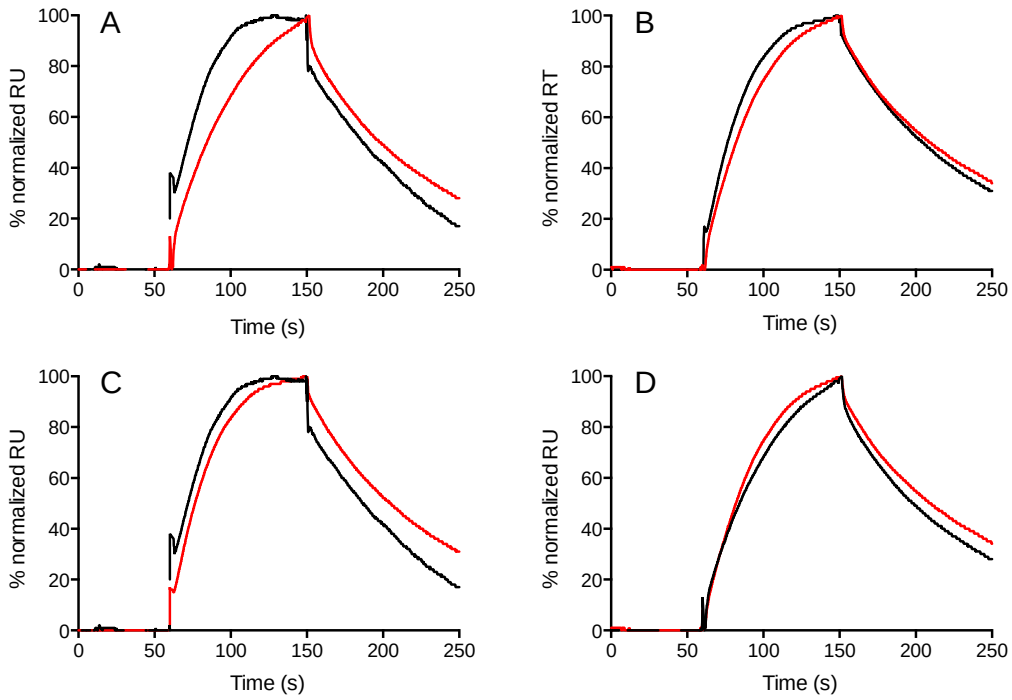

Supplemental Figure 8: Surface plasmon resonance (SPR) experiments. Binding of 1 and 2 to CA coated surfaces measured by SPR. (A) SPR sensogram of compound 1 on immobilized CAIX (black) and immobilized CAII (red). (B) SPR sensogram of reference acetazolamide on immobilized CAIX (black) and immobilized CAII (red). (C) SPR sensogram on immobilized CAIX for compound 1 (black) and reference acetazolamide (red). (D) SPR sensogram on immobilized CAII for compound 1 (black) and reference acetazolamide (red).

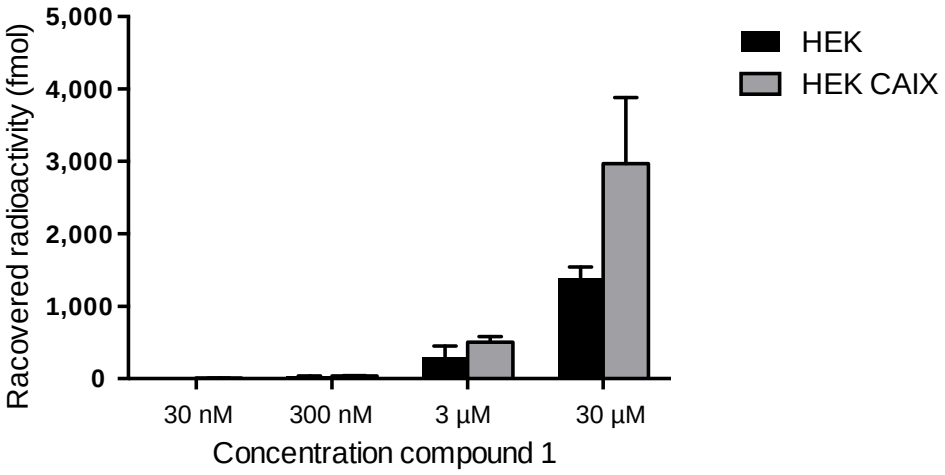

Supplemental Figure 9: *In vitro* cell binding experiment. HEK EBNA 293 cells (black bars) and HEK EBNA 293 cells transfected with the full-length CAIX protein (*4*) (grey bars, 1.5 × 105 cells per sample, in duplicate) were incubated in TBS Buffer for 15 min at room temperature with a ^{99m}Tc-labeled compound 1 at concentrations ranging from 30 nM to 30 □M. The cells were washed and counted in a Packard Cobra γ-counter. Results are plotted as average recovered radioactivity ± standard deviation. The difference at 30 µM is statistically significant (Student t-Test, $p < 0.05$)

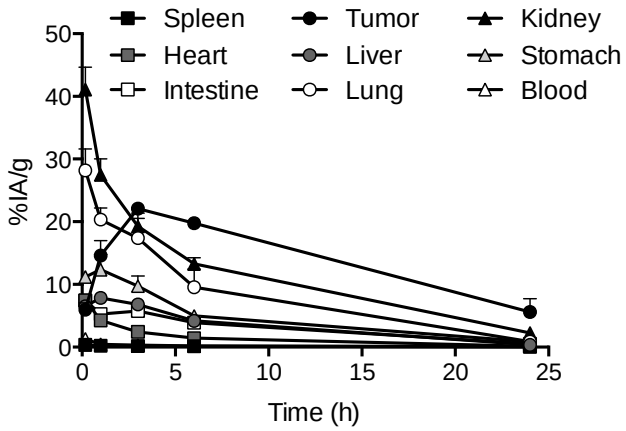

Supplemental Figure 10: Time course profile and tissue distribution of ^{99m}Tc-labeled preparations of compound 1. Mean values ± standard deviation are plotted over time.

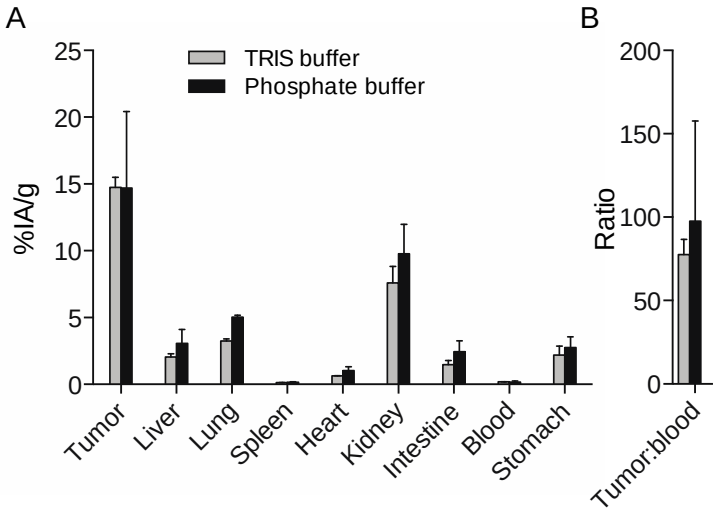

Supplemental Figure 11: Influence of dilution buffer on the biodistribution profile. ^{99m}Tc-labeled preparations of 1 were diluted to the final concentration of 12.5 µg/kg either in Phosphate (black bars) or TRIS (grey bars) Buffer solutions prior to injection into SKRC-52 tumor bearing mice. Both the biodistribution profiles (A) and ratios between tumor and blood (B) confirm that the two buffers do not significantly impact on the capacity of the AAZ-derived CAIX binding molecule to significantly accumulate at the tumor site 6 hours post injection.

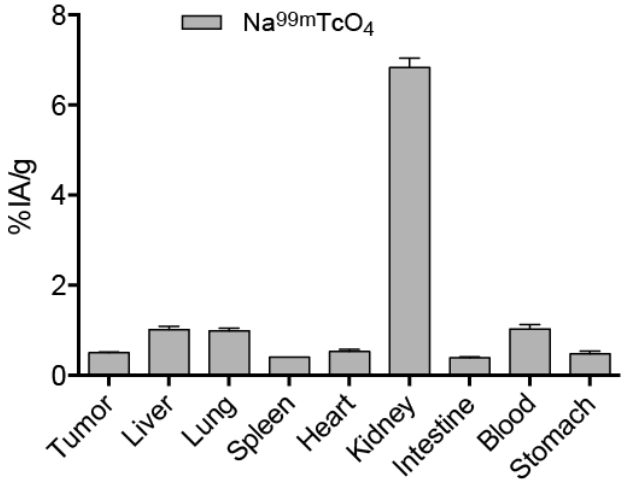

Supplemental Figure 12: Quantitative biodistribution of $Na^{99m}TcO_4$ three hours after intravenous injection in SKRC-52 tumor bearing mice. The radionuclide is rapidly excreted through the kidney and no significant accumulation can be detected in the tumor.

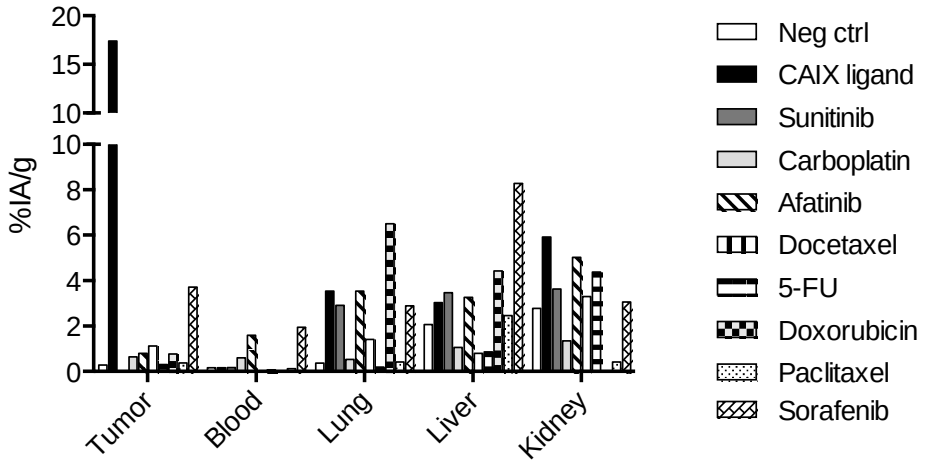

Supplemental Figure 13: Comparison between a ^{99m}Tc-chelating AAZ derivative over published biodistribution data of approved small molecule drugs (*5-12*). The reported data refer to organ distributions at 6 hours post injection; in the case these values were not available, they were extrapolated from the experimental data by power function fitting.

Experiment	*Figure*	*Compound*	*Labeling activity*	*Specific activity*	*Injected dose*	*Injected activity*
Time course	**2**	**1**	276 MBq	4.5 MBq/nmol	13 µg/kg 14 nmol/kg	1.4 MBq
"	"	**2**	175 MBq	2.9 MBq/nmol	13 µg/kg 17 nmol/kg	0.9 MBq
Dose dependence	**3**	**1**	223 MBq	3.6 MBq/nmol	2.5 µg/kg 2.8 nmol/kg	0.2 MBq
"	"	"	"	"	13 µg/kg 14 nmol/kg	1.1 MBq
"	"	"	"	"	25 µg/kg 28 nmol/kog	2.2 MBq
"	"	"	"	"	65 µg/kg 74 nmol/kg	5.8 MBq
Pre injection with unlabeled **1**	"	**1**	135 MBq	2.2 MBq/nmol	40 µg/kg 45 nmol/kg	2.2 MBq

Supplemental Table 1: Labeling and average injection activities used in different experiments

	10 min		*1 h*		*3 h*		*6 h*		*24 h*	
Tissues (% IA/g)	***1***	***2***	***1***	***2***	***1***	***2***	***1***	***2***	***1***	***2***
Tumor	5.97 (± 1.09)	1.85 (± 0.36)	14.60 (± 2.39)	0.26 (± 0.03)	22.11 (± 0.61)	0.16 (± 0.01)	19.77 (± 0.87)	0.13 (± 0.01)	5.59 (± 2.13)	0.10 (± 0.02)
Liver	6.51 (± 0.21)	3.25 (± 0.62)	7.86 (± 0.82)	1.71 (± 0.14)	6.83 (± 0.84)	0.79 (± 0.02)	4.19 (± 0.64)	0.43 (± 0.07)	0.37 (± 0.15)	0.19 (± 0.04)
Lung	28.17 (± 3.43)	4.85 (± 1.38)	20.36 (± 1.82)	0.52 (± 0.05)	17.38 (± 3.12)	0.22 (± 0.01)	9.57 (± 2.89)	0.16 (± 0.01)	0.90 (± 0.39)	0.11 (± 0.02)
Spleen	0.36 (± 0.06)	1.00 (± 0.20)	0.22 (± 0.02)	0.17 (± 0.02)	0.19 (± 0.05)	0.13 (± 0.01)	0.14 (± 0.03)	0.12 (± 0.02)	0.07 (± 0.02)	0.10 (± 0.02)
Heart	7.46 (± 0.81)	2.33 (± 0.96)	4.26 (± 0.25)	0.26 (± 0.03)	2.45 (± 0.09)	0.12 (± 0.01)	1.42 (± 0.33)	0.09 (± 0.01)	0.15 (± 0.07)	0.05 (± 0.01)
Kidney	41.12 (± 3.57)	11.02 (± 2.79)	27.47 (± 2.53)	2.44 (± 0.42)	19.28 (± 2.14)	2.20 (± 0.24)	13.29 (± 1.04)	2.12 (± 0.28)	2.28 (± 0.84)	1.36 (± 0.36)
Intestine	7.42 (± 0.46)	1.32 (± 0.31)	5.29 (± 0.60)	0.63 (± 0.17)	5.75 (± 0.81)	0.27 (± 0.12)	3.88 (± 0.76)	0.13 (± 0.04)	0.54 (± 0.17)	0.06 (± 0.01)
Stomach	11.19 (± 0.78)	2.05 (± 0.55)	12.36 (± 2.43)	0.39 (± 0.15)	9.71 (± 1.65)	0.27 (± 0.04)	4.99 (± 0.21)	0.17 (± 0.03)	0.87 (± 0.52)	0.12 (± 0.03)
Blood	1.30 (± 0.29)	5.08 (± 0.75)	0.45 (± 0.03)	0.47 (± 0.06)	0.32 (± 0.03)	0.21 (± 0.01)	0.20 (± 0.01)	0.14 (± 0.01)	0.09 (± 0.02)	0.06 (± 0.0)
Tumor:blood	4.89 (± 1.93)	0.36 (± 0.02)	32.82 (± 6.94)	0.56 (± 0.04)	69.86 (± 6.16)	0.21 (± 0.01)	100.61 (± 8.37)	0.94 (± 0.06)	68.33 (± 34.63)	1.55 (± 0.20)

Supplemental Table 2: Organ distribution of radioactivity following single-dose intravenous administration of radiolabeled preparation of compounds 1 and 2 in SKRC-52 bearing mice at different time point. The values presented are the mean ± standard deviation of three mice.

Tissues (% IA/g)	*2.5 µg/kg 2.8 nmol/kg*	*13 µg/kg 14 nmol/kg*	*25 µg/kg 28 nmol/kg*	*65 µg/kg 74 nmol/kg*
Tumor	14.2 (± 3.16)	14.70 (± 5.73)	17.42 (± 2.39)	12.26 (± 1.62)
Liver	3.02 (± 0.29)	3.07 (± 1.05)	3.03 (± 0.49)	1.73 (± 0.63)
Lung	5.95 (± 0.58)	5.04 (± 0.14)	3.54 (± 0.53)	0.83 (± 0.24)
Spleen	0.15 (± 0.01)	0.15 (± 0.04)	0.16 (± 0.01)	0.11 (± 0.02)
Heart	1.21 (± 0.16)	1.03 (± 0.30)	0.65 (± 0.12)	0.27 (± 0.07)
Kidney	11.76 (± 1.38)	9.79 (± 2.20)	5.92 (± 0.50)	4.71 (± 1.03)
Intestine	3.02 (± 0.63)	2.45 (± 0.81)	1.17 (± 0.16)	1.26 (± 0.75)
Stomach	3.44 (± 0.16)	2.76 (± 0.80)	1.70 (± 0.19)	1.01 (± 0.28)
Blood	0.18 (± 0.09)	0.18 (± 0.09)	0.17 (± 0.19)	0.18 (± 0.02)
Tumor:blood	103.25 (± 66.02)	97.58 (± 60.00)	101.41 (± 13.62)	67.86 (± 0.61)

Supplemental Table 3: Organ distribution of radioactivity after 3 hours following intravenous administration of different doses of radiolabeled preparation of compound 1 in SKRC-52 bearing mice. The values presented are the mean ± standard deviation of three mice.

Supplemental References

1. Chan TR, Hilgraf R, Sharpless KB, Fokin VV. Polytriazoles as copper(I)-stabilizing ligands in catalysis. *Org Lett.* 2004;6:2853-2855.

(renumber rest of references and callouts)

3. Reddy JA, Xu LC, Parker N, Vetzel M, Leamon CP. Preclinical evaluation of (99m)Tc-EC20 for imaging folate receptor-positive tumors. *J Nucl Med.* 2004;45:857-866.

4. Ahlskog JK, Dumelin CE, Trussel S, Marlind J, Neri D. In vivo targeting of tumor-associated carbonic anhydrases using acetazolamide derivatives. *Bioorg Med Chem Lett.* 2009;19:4851-4856.

5. Abe Y, Fukuda H, Ishiwata K, et al. Studies on 18F-labeled pyrimidines. Tumor uptakes of 18F-5-fluorouracil, 18F-5-fluorouridine, and 18F-5-fluorodeoxyuridine in animals. *Eur J Nucl Med.* 1983;8:258-261.

6. Poot AJ, van der Wildt B, Stigter-van Walsum M, et al. [(1)(1)C]Sorafenib: radiosynthesis and preclinical evaluation in tumor-bearing mice of a new TKI-PET tracer. *Nucl Med Biol.* 2013;40:488-497.

7. Slobbe P, Windhorst AD, Stigter-van Walsum M, et al. Development of [18F]afatinib as new TKI-PET tracer for EGFR positive tumors. *Nucl Med Biol.* 2014;41:749-757.

8. Zhao X, Zhao Y, Geng L, et al. Pharmacokinetics and tissue distribution of docetaxel by liquid chromatography-mass spectrometry: evaluation of folate receptor-targeting amphiphilic copolymer modified nanostructured lipid carrier. *J Chromatogr B Analyt Technol Biomed Life Sci.* 2011;879:3721-3727.

9. Bosslet K, Straub R, Blumrich M, et al. Elucidation of the mechanism enabling tumor selective prodrug monotherapy. *Cancer Res.* 1998;58:1195-1201.

10. Cao Q, Li ZB, Chen K, et al. Evaluation of biodistribution and anti-tumor effect of a dimeric RGD peptide-paclitaxel conjugate in mice with breast cancer. *Eur J Nucl Med Mol Imaging.* 2008;35:1489-1498.

11. Kim YS, Song R, Hyun Kim D, Jun MJ, Sohn YS. Synthesis, biodistribution and antitumor activity of hematoporphyrin-platinum(II) conjugates. *Bioorg Med Chem.* 2003;11:1753-1760.

12. Kuchar M, Oliveira MC, Gano L, Santos I, Kniess T. Radioiodinated sunitinib as a potential radiotracer for imaging angiogenesis-radiosynthesis and first radiopharmacological evaluation of 5-[125I]Iodo-sunitinib. *Bioorg Med Chem Lett.* 2012;22:2850-2855.